06.5

Phase Transformations in Stainless Cr-Mn-N Steel Activated by Nanostructuring Surface Treatment and Their Influence on Deformation Behavior and Fracture at Cryogenic Temperatures

© N.A. Narkevich, E.E. Deryugin, I.V. Vlasov

Institute of Strength Physics and Materials Science, Siberian Branch, Russian Academy of Sciences, Tomsk, Russia
E-mail: natnark@list.ru

Received January 25, 2022
Revised March 9, 2022
Accepted March 11, 2022.

The structure of stainless austenitic Cr−Mn−N steel after deformation treatment of its surface by ultrasonic forging strain (UFS) has been studied. It is shown that UFS activates strain aging in the near-surface layer with the formation of CrN particles. Preliminary ultrasonic treatment of the steel surface contributes to an increase in the yield strength during tensile tests at a temperature of −196°C and provides ductile fracture of the near-surface layer.

Keywords: high nitrogen steel, austenite, ultrasonic forgingstrain, strain aging, cryogenic temperature, martensitic transformation.

DOI: 10.21883/TPL.2022.05.53469.19145

Strain dispersion of the structure of metals and alloys to nanoscale state can significantly improve their physical and mechanical characteristics [1–4]. The structures formed by large and megaplastic strains are quite unusual. Reduction in size of metals and alloys structure to the nanoscale level according to [5] prevents nucleation and propagation of cracks. The boundaries of strain fragments in such a structure during subsequent annealing are not capable of active migration [6]. In aging steels Cg−Mn−N during severe plastic strain primary nitrides may dissolve, and secondary dispersion hardening may take place [7].

Interest in the surface hardening of metallic materials [3,4,8] by severe strain is due to a combination of technological simplicity with the effectiveness of increasing strength characteristics. These methods are promising for active application in order to harden the near-surface layers of austenitic steels with low packing defect energy. Representatives of this class of steels are nickel-free austenitic high-nitrogen steels. They have high strain hardening, demonstrate high strength, ductility and fracture toughness, including at negative temperatures (up to cryogenic) [4,9]. However, the effect of structure dispersion on the strain behavior and fracture nature at cryogenic temperatures in relation to the phase transformations occurring during both nanostructured pretreatment and subsequent low-temperature strain has not been investigated. To develop previously published papers [8,9], it is of interest to study the indicated aspects on the example of Cr−Mn−N steel.

Steel was melted in a 50-kg induction furnace with a chromium-magnesite lining. Armco-iron, low-carbon ferrochrome, metallic manganese, and nitrided ferrochrome were used as a charge. The chemical composition of the investigated Cr−Mn−N steel is shown in the table.

Chemical composition (in wt.%)

Cr	Mn	Si	Ni	C	N	P	S	Fe
16.50	18.81	0.52	0.24	0.07	0.53	0.01	0.001	Res.

After tempering from 1100°C in water, steel had single-phase large-crystal austenitic structure with grain size 30−50 μm. The surface of the steel plate with thickness of 10 mm, width of 20 mm and length of 100 mm was ground and polished with diamond pastes. Then the surface was treated by forging with ultrasonic frequency (ultrasonic forge treatment) at room temperature on equipment and using the method described in [3]. Samples were cut from this plate using spark erosion with working area dimensions of 15×2.5 mm and thickness of 1 mm. In the samples for mechanical testing only one surface was subjected to ultrasonic forge treatment. The thickness of the hardened layer was 10% of the sample thickness.

The structure of the near-surface layer of steel was examined with a transmission electron microscope HT-7700 (TEM) (Hitachi, Japan) at accelerating voltage of 120 kV. Cross sections were made using a system of focused ion beam FB-2100 (Hitachi, Japan).

Mechanical strain tests were conducted on a test machine INSTRON 5582 (USA) at temperature of −196°C with speed of $1.87 \cdot 10^{-4}\,s^{-1}$ until destruction. Samples after tempering were used for comparison under the same conditions.

The destruction surface structure was investigated on a raster electron microscope Tescan MIRA 3 LMU.

Highly dispersed fragmented structure of austenite after ultrasonic forge treatment is characterized with a ring

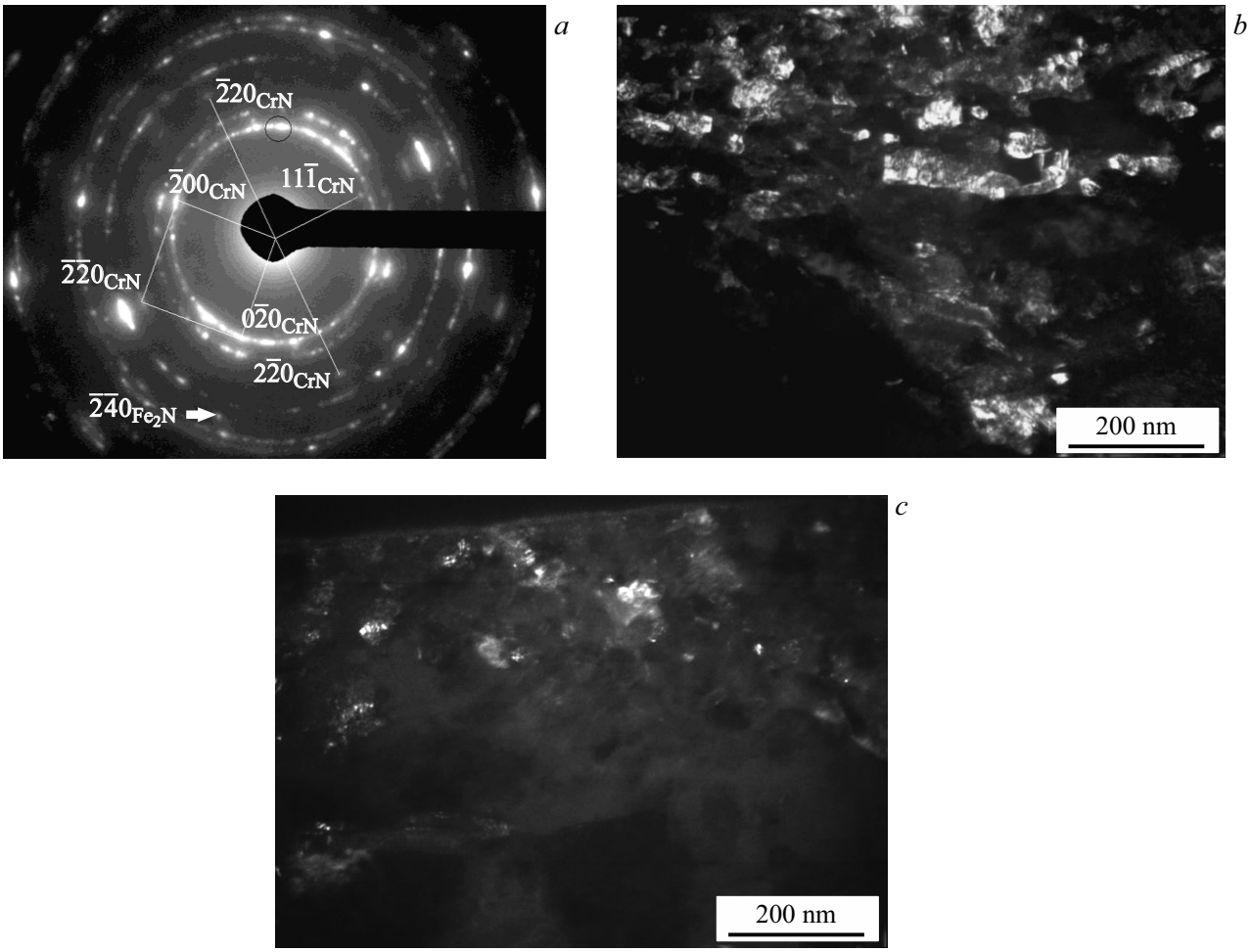

Figure 1. Structure of near-surface layer of steel Cr−Mn−N after ultrasonic forge treatment. *a* — electron diffraction pattern with reflex lattices CrN: $z = [112]$ and $[001]$; *b* — dark field image of the structure in a ring fragment $(111)_\gamma$, identified by a selector diaphragm on the electron diffraction pattern, shown in part *a*; *c* — dark-field image of the structure in reflex $(11\bar{1})_{CrN}$.

electron diffraction pattern with continuous and discrete misorientations (fig. 1, *a*).

The size of fragments in austenitic structure of near surface layer shown in fig. 1, *b*, does not exceed 30 nm. Apart from rings, the electron diffraction pattern also includes reflexes of other phases with interplanar distances different from those present in austenite. Some of them form reflex nets. One of nets with the axis of zone [112] is shown in fig.1, *a*. By the value of interplanar distances and angle between the directions, the phase is identified as nitride CrN ($d_{(111)} = 2.40$ Å, $d_{(220)} = 1.46$ Å) with a face-centered cubic lattice. Dark-field image of the structure in the reflex $(11\bar{1})_{CrN}$ shows brightly luminous nitrides with size of 1−3 nm (fig. 1, *c*). There are also areas with the size of up to 10 nm. The other net is formed by reflexes related to the axis of the zone $[001]_{CrN}$ (fig. 1, *a*), which separately accommodates a reflex $(\bar{2}20)_{CrN}$, and reflexes of type $\{200\}_{CrN}$ are located in a ring $\{111\}_\gamma$, since corresponding crystallographic planes of nitride and austenite have close interplanar distances ($d_{(111)\gamma} = 2.08$ Å, $d_{(200)CrN} = 2.07$ Å). The electron diffraction pattern also includes reflexes of other nitride, for example Fe_2N.

Therefore, analysis of electron diffraction pattern and dark field images demonstrated that strain treatment at 23°C activate strain ageing in a dispersed austenite structure of near-surface layer. The paper [10] demonstrates that formation of coherent precipitations of CrN in steel with similar composition occurs at thermal treatment — ageing at 500°C for 2 h. Formation of CrN during cold strain ultrasonic forge treatment indicates, firstly, the highly non-equilibrium state of the nitrogen-doped solid solution and, secondly, that strain ageing in this case is the mechanism of relaxation of the internal stresses formed during ultrasonic forge treatment. The relaxation process is evidenced by the fact that the volume of the CrN face-centered cubic lattice is larger than that of the matrix phase. Consequently, they are formed in local regions of tensile stresses.

The papers [4,8] demonstrated that there is no HPC lattice martensite in the near-surface layer after strain treatment ε. The reason for that is strain heating causing reverse $\varepsilon \rightarrow \gamma$-

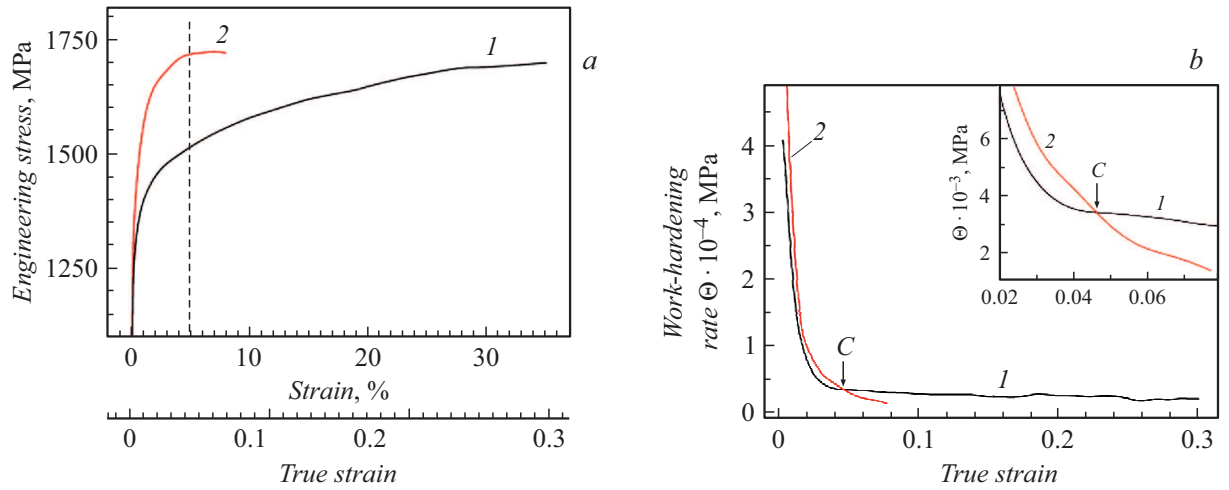

Figure 2. Curves $\sigma-\varepsilon$ (a) and charge in strain hardening rate (b) in strain tests at -196°C for steel Cr–Mn–N after tempering from 1100°C (*1*) and after ultrasonic forge treatment (*2*).

transformation [8] in process of treatment. The intensity of strain heating is low, since a thick (10 mm) plate in process of ultrasonic forge treatment was heated by not more than to 50°C. In local microvolumes the temperature was higher, and this factor additionally supported precipitation of dispersed nitride particles. At a larger depth the impact of strain heating weakens, and ε-martensite [4] is observed in the structure inside the strain twins.

It is well known [1] that in the limited deformed state the metal materials have low plasticity. Plasticity and viscosity of damage become even lower at negative strain temperatures [9,11]. One of the reasons for that is strain induce $\gamma \rightarrow \varepsilon$-transformation [9] or $\gamma \rightarrow \varepsilon \rightarrow \alpha$-transformation. The full cycle $\gamma \rightarrow \varepsilon \rightarrow \alpha$-transformation was observed in the zone of investigated steel strain localization immediately prior to damage at -196°C [3]. Indeed, the plasticity of samples with the strengthened surface layer is substantially lower than without it (fig. 2, a).

It is obvious that ultrasonic forge treatment increases yield strength, but does not impact the tensile strength. Obviously, increase in yield strength is due to the high resistance to strain of the near-surface layer with nanostructure and the strength value is determined by the structure of 90% of the sample thickness outside the hardened near-surface layer. The moment when this layer ceases to act as a barrier to tensile plastic strain and collapses, corresponds to strain $\varepsilon_{true} = 0.046$ at point C in fig. 2, b. To the right of this point, the strain-hardening rate of the sample with the nanostructured layer becomes less than the corresponding characteristic of the untreated sample.

The work of plastic strain, at which the strain $\varepsilon_{true} = 0.046$ determined by the area bounded by the curve *2* in fig. 2, a, is 13% greater than the corresponding value for the curve *1*. An increase in strain above this value leads to a decrease in the strain hardening rate compared to the sample without the nanostructured layer. Thus, the experimental results indicate that the ultrasonic forge treatment of the investigated steel reduces its ductility, but at the same time the ductility of the nanostructured layer before its fracture is high enough ($\sim$ 5%). Consequently, the decrease of relative elongation in samples with nanostructured layer occurs due to the peculiarities of structure changes in the sample cross-section outside this layer.

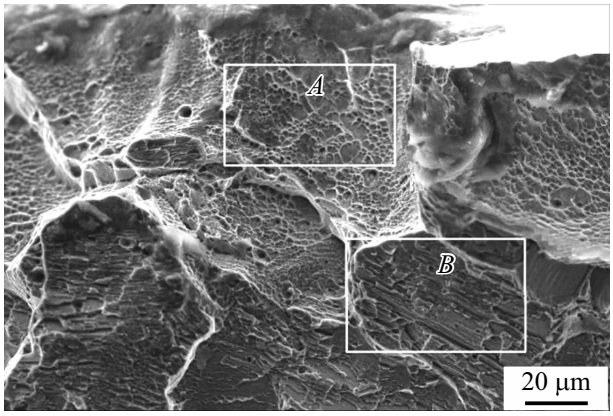

Figure 3. Fractographic image of Cr–Mn–N steel fracture with the surface exposed to prior ultrasonic forge treatment and tested for tensile strength at -196°C. *A* — viscous fracture, *B* — brittle fracture.

The study of the surface of the destroyed specimens revealed the difference in the micromechanisms of near-surface nanodispersed layer fracture containing CrN particles and the rest of the sample cross section (fig. 3).

The near-surface layer with dispersed nanoscale structure in high-nitrogen austenitic Cr–Mn–N steel during subsequent deformation at -196°C fractures viscously. Outside of this layer the steel fracture is brittle. The fracture has a specific lamellar structure. ε-martensite with HPC lattice [9,12] is responsible for such fracture.

Therefore, ultrasonic forge treatment helps to form CrN particles in near surface layer and to improve yield strength. Besides, after ultrasonic forge treatment at room temperature and subsequent tensile strength tests at -196°C, absence of ε-martensite with HPC lattice in the near surface layer was noted, which provides for its viscous nature of fracture.

Acknowledgments

Structural research was carried out using the equipment provided by the Krasnoyarsk Regional Center for Collective Use, Federal Research Center, Krasnoyarsk Scientific Center of the Siberian Branch of the Russian Academy of Sciences.

Funding

This study was supported financially by the Russian Science Foundation (grant № 22-29-00438).

Conflict of interest

The authors declare that they have no conflict of interest.

References

[1] R.Z. Valiev, Yu. Estrin, Z. Horita, T.G. Langdon, M.J. Zechetbauer, Yu.T. Zhu, JOM, **58** (4), 33 (2006). DOI: 10.1007/s11837-006-0213-7
[2] J.W. Bae, P. Asghari-Rad, A. Amanov, H.S. Kim, Mater. Sci. Eng. A, **826**, 141966 (2021). DOI: 10.1016/j.msea.2021.141966
[3] N.A. Narkevich, A.I. Tolmachev, I.V. Vlasov, N.S. Surikova, Phys. Met. Metallogr., **117** (3), 288 (2016). DOI: 10.1134/S0031918X16030108.
[4] N.A. Narkevich, E.E. Deryugin, O.B. Perevalova, I.V. Vlasov, Mater. Sci. Eng. A, **834**, 142590 (2022). DOI: 10.1016/j.msea.2021.142590
[5] Yu.R. Kolobov, S.S. Manokhin, V.I. Betekhtin, A.G. Kadomtsev, M.V. Narykova, G.V. Odintsova, G.V. Khramov, Pisma v ZhTF, **48** (2), 15 (2022) (in Russian). DOI: 10.21883/PJTF.2022.02.51913.19025
[6] A.M. Glezer, A.A. Tomchuk, V.I. Betekhtin, B. Dunsue, Tech. Phys. Lett., **43** (4), 399 (2017). DOI: 10.1134/S1063785017040216.
[7] V. Shabashov, K. Lyashkov, K. Kozlov, V. Zavalishin, A. Zamatovskii, N. Kataeva, V. Sagaradze, Yu. Ustyugov, Materials, **14**, 7116 (2021). DOI: 10.3390/ma14237116
[8] V.V. Sagaradze, N.V. Kataeva, I.G. Kabanova, S.V. Afanasev, A.V. Pavlenko, Phys. Met. Metallogr., **121** (7), 683 (2020). DOI: 10.1134/S0031918X20070091.
[9] N. Narkevich, Ye. Deryugin, Yu. Mironov, Metals, **11** (5), 710 (2021). DOI: 10.3390/met11050710
[10] V.V. Berezovskaya, Yu.A. Raskovalova, E.A. Merkushkin, R.Z. Valiev, Met. Sci. Heat Treat., **57** (11-12), 656 (2016). DOI: 10.1007/s11041-016-9938-2.
[11] S.A. Vologzhanina, B.S. Ermakov, A.A. Peregudov, IOP Conf. Ser.: Earth Environ. Sci., **459** (6), 062118 (2020). DOI: 10.1088/1755-1315/459/6/062118
[12] N.A. Narkevich, N.S. Surikova, Phys. Met. Metallogr., **121** (12), 1175 (2020). DOI: 10.1134/S0031918X2012008X.